

UC San Diego

UC San Diego Previously Published Works

Title

Application of Hysteretic Trends in the Preconsolidation Stress of Unsaturated Soils

Permalink

<https://escholarship.org/uc/item/3fx725sk>

Journal

Geotechnical and Geological Engineering, 36(1)

ISSN

0960-3182

Authors

Mun, W

Coccia, CJR

McCartney, JS

Publication Date

2018-02-01

DOI

10.1007/s10706-017-0316-7

Peer reviewed

[Click here to view linked References](#)

1
2
3
4 1 **APPLICATION OF HYSTERETIC TRENDS IN THE PRECONSOLIDATION STRESS**
5
6 2 **OF UNSATURATED SOILS**

7
8
9 3 **By W. Mun, Ph.D.¹, C.J.R. Coccia, Ph.D.², and J.S. McCartney, Ph.D., P.E.³**

10
11 4 **ABSTRACT:** This paper involves an evaluation of a relationship describing the evolution in yield
12
13
14 5 stress of unsaturated soils during hydraulic hysteresis, and an application of this relationship in an
15
16 6 elasto-plastic framework to predict the compression curves of unsaturated soils under drained (free
17
18 7 outflow of air and water with constant suction) or undrained (constant water content with no
19
20 8 outflow of water and varying suction) conditions. The yield stress was quantified as the apparent
21
22 9 mean effective preconsolidation stress obtained from compression tests reported in the literature
23
24 10 on specimens that had experienced different hydraulic paths. It was observed that the
25
26 11 preconsolidation stress does not follow a hysteretic path when plotted as a function of matric
27
28 12 suction, but does when plotted as a function of the degree of saturation. Accordingly, an existing
29
30 13 logarithmic relationship between the preconsolidation stress and matric suction normalized by the
31
32 14 air entry suction was found to match the experimental preconsolidation stress results. This same
33
34 15 relationship was also able to satisfactorily predict the trends in preconsolidation stress with degree
35
36 16 of saturation by substituting the hysteretic soil-water retention curve (SWRC) into the place of the
37
38 17 matric suction. The relationship between preconsolidation stress and suction was combined with
39
40 18 an elasto-plastic framework to predict the compression curves of soils during drained compression,
41
42 19 while the wetting-path relationship between preconsolidation stress and degree of saturation was
43
44
45
46
47
48
49
50
51
52

53
54
55 ¹ Senior Staff Engineering, Converse Consultants, 717 South Myrtle Ave., Monrovia, CA 91016,
56 woongju.mun@gmail.com

57 ² Associate, Exponent Failure Analysis Associates, 1331 17th St, Suite 515, Denver, CO 80202,
58 ccoccia@exponent.com

59 ³ Associate Professor, Dept. of Structural Eng., Univ. of California San Diego, 9500 Gilman Dr., La Jolla, CA
60 92093-0085; mccartney@ucsd.edu

1
2
3
4
5
6
7
8
9
10
11
12
13
14
15
16
17
18
19
20
21
22
23
24
25
26
27
28
29
30
31
32
33
34
35
36
37
38
39
40
41
42
43
44
45
46
47
48
49
50
51
52
53
54
55
56
57
58
59
60
61
62
63
64
65

20 combined with the framework to predict the compression curves of soils during undrained
21 (constant water content) compression. A good match was obtained with experimental data from
22 the literature, indicating the relevance of considering the hysteretic SWRC and preconsolidation
23 relationships when simulating the behavior of unsaturated soils following different hydro-
24 mechanical paths.

INTRODUCTION

26 Several hydro-mechanical, elasto-plastic frameworks have been developed to simulate the
27 impacts of changes in mean total or effective stress and matric suction on the volume change of
28 unsaturated soils. The ability of these frameworks to predict the hydro-mechanical behavior of
29 unsaturated soil is influenced by the stress state definition. While early studies extended the critical
30 state framework to unsaturated soils using independent state variables (Alonso et al. 1990; Wheeler
31 and Sivakumar 1995; Cui and Delage 1996), other studies used the generalized effective stress
32 concept (Loret and Khalili 200; Gallipoli et al. 2003; Wheeler et al. 2003; Tamagnini 2004;
33 Romero and Jommi 2008; Khalili et al. 2008; Della Vecchia et al. 2013). An advantage of using
34 the generalized effective stress concept is that a smaller number of material properties may be
35 needed to simulate the complex volume change behavior of unsaturated soils, and the yield surface
36 will always be concave and thermodynamically consistent (Khalili et al. 2008). Further, the effects
37 of hydraulic hysteresis may be considered in an elasto-plastic framework by incorporating the soil-
38 water retention curve (SWRC) (Wheeler et al. 2003; Tamagnini 2004) or the air entry suction
39 (Khalili et al. 2008) in the definition of the generalized effective stress concept. Using the
40 generalized effective stress concept, this study involves an evaluation of how the SWRC can also
41 be incorporated into the definition of the yield stress in hydro-mechanical frameworks to consider
42 the effects of hydraulic hysteresis on this parameter.

1
2
3
4 43 A common feature of most hydro-mechanical elasto-plastic frameworks is the evolution in
5
6 44 yield stress with matric suction, commonly referred to as the loading-collapse (LC) curve. The
7
8
9 45 Barcelona Basic Model (BBM) presented by Alonso et al. (1990) is one of the most widely used
10
11 46 models for unsaturated soils in terms of independent stress state variables. Although the BBM is
12
13
14 47 capable of considering suction hardening behavior (e.g., increase in the preconsolidation stress
15
16 48 with suction increasing) and expansion and collapse phenomena, problems have been encountered
17
18
19 49 in matching the model to experimental data (Wheeler et al. 2002), and there may be issues
20
21 50 considering the behavior of soils under suctions less than the air entry suction. Despite the fact that
22
23
24 51 the concept of the LC curve is well-established, limited experimental data sets are available to
25
26 52 thoroughly evaluate the influence of suction and degree of saturation on the mean effective
27
28
29 53 preconsolidation stress of unsaturated soils. Specifically, knowledge of the SWRC or monitoring
30
31 54 of the degree of saturation and/or suction during compression is needed to estimate the mean
32
33 55 effective preconsolidation stress (Salager et al. 2008; Uchaipichat and Khalili 2009; Uchaipichat
34
35
36 56 2010; Coccia 2016; Khosravi et al. 2016). This study seeks to develop and validate a simple
37
38 57 hysteretic relationship between the mean effective preconsolidation stress p'_c , matric suction ψ ,
39
40
41 58 and degree of saturation S_r using the limited sets of data that are available in the literature.
42
43 59 Following this, the new relationship is employed to as part of a simple hydro-mechanical
44
45
46 60 framework to predict the volume change behavior of unsaturated soils under different drainage
47
48 61 conditions.

62 **BACKGROUND**

63 The LC curve is used to indicate the yield limit transition from an elastic to an elasto-plastic
64
65 volumetric soil response during compression of unsaturated soils. Under isotropic stress states, the
66
67 yield limit of soils is typically assumed to be equal to the mean effective preconsolidation stress

1
2
3
4 66 (Wood 1990), although for unsaturated soils it has been defined in terms of the mean net
5
6 67 preconsolidation stress $p_{c,net}$ or the mean effective preconsolidation stress p'_c depending on the
7
8
9 68 choice of stress state variables. This paper is focused on isotropic loading, so all further discussion
10
11 69 of preconsolidation stress are for the mean preconsolidation stress. In general, most LC curves
12
13
14 70 indicate an increase in preconsolidation stress with increasing matric suction, an effect commonly
15
16 71 referred to as “suction hardening”, albeit with different shapes for this relationship. Analytical
17
18
19 72 expressions to characterize the LC curve for unsaturated soils have been proposed in the literature
20
21 73 in p_{net} vs. suction (ψ) space (Alonso et al. 1990), p' vs. ψ space (Salager et al. 2008; Tourchi and
22
23
24 74 Hamidi 2015), p' vs. degree of saturation (S_r) space (Gallipoli et al. 2003; Romero and Jommi
25
26 75 2008), p' vs. modified suction space (i.e., suction multiplied by the porosity $\psi \cdot n$) (Wheeler et al.
27
28
29 76 2003), and p' vs. effective saturation (S_e) space (Zhou et al. 2012b). The shapes of some typical
30
31 77 LC curves are shown in Figure 1, along with their analytical expressions. Several studies have
32
33
34 78 defined the evolution of p'_c with changes in matric suction (Lloret et al. 2003; Geiser et al. 2006;
35
36 79 Salager et al. 2008; Uchaipichat and Khalili 2009; Mun and McCartney 2015, 2016; Khosravi et
37
38
39 80 al. 2016), which have all confirmed an increasing trend between p'_c and matric suction during
40
41 81 drying. Alsherif and McCartney (2016) found that a similar increasing trend may also be present
42
43
44 82 at high suction magnitudes. Although the suction is clearly related to p'_c , the evolution in p'_c may
45
46 83 also be related to changes in soil structure during application of suction to the soil or due to
47
48
49 84 different distributions in water throughout the soil during wetting and drying (hydraulic
50
51 85 hysteresis).

52
53 86 A well-known LC curve is that of Alonso et al. (1990), which was formulated to link the
54
55
56 87 relationship between the preconsolidation stress and suction with the slope of the virgin
57
58 88 compression line in net mean stress space. The LC curve proposed by Alonso et al. (1990) with a

1
2
3
4
5
6
7
8
9
10
11
12
13
14
15
16
17
18
19
20
21
22
23
24
25
26
27
28
29
30
31
32
33
34
35
36
37
38
39
40
41
42
43
44
45
46
47
48
49
50
51
52
53
54
55
56
57
58
59
60
61
62
63
64
65

89 hypothetical hydro-mechanical loading path for an overconsolidated soil subjected to an increase
90 in matric suction followed by an increase in mean net stress is shown in Figure 1(a) in $p_{net} - \psi$
91 space. As matric suction increases, the soil is assumed to behave elastically along path O→A while
92 the stress state remains within the LC curve. During this increase in suction, an apparent increase
93 in p_c will also occur as defined by the LC curve (Figure 1(a)). An increase in net stress along path
94 A→B will also result in an elastic response until reaching the LC curve at point B. Further increases
95 in mean net stress result in an elasto-plastic response, along with expansion of the LC curve due
96 to stress-induced hardening. Although this loading path is the focus of this study, plastic strains
97 may also be generated along other paths in the elasto-plastic frameworks for unsaturated soils that
98 consider coupling between hydraulic and mechanical loading paths (Wheeler et al. 2003; Romero
99 and Jommi 2008). The other LC curves presented in Figure 1 function in a similar way to that of
100 Alonso et al. (1990), but interpret LC curve in terms of the mean effective preconsolidation stress.
101 The relationship of Wheeler et al. (2003) also permits coupling between mechanical and hydraulic
102 loading paths to be considered by incorporating suction increase (SI) and suction decrease (SD)
103 curves that bound the region of elastic response.

104 An advantage of the framework of Alonso et al. (1990) is that it can predict wetting-induced
105 swelling or collapse of unsaturated soils. In this case, the slope of the virgin compression line in
106 mean net stress space decreases with suction in order to predict collapse. However, this change in
107 the slope of the virgin compression line with suction is not necessarily observed when interpreting
108 soil behavior in terms of generalized effective stress (Uchaipichat and Khalili 2009), and the
109 decrease in slope may lead to problems when trying to predict the phenomenon of pressurized
110 saturation during drained compression to high mean stresses (Mun and McCartney 2015, 2016).
111 Mun and McCartney (2016) found that the slope of the virgin compression line of an unsaturated

1
2
3
4
5
6
7
8
9
10
11
12
13
14
15
16
17
18
19
20
21
22
23
24
25
26
27
28
29
30
31
32
33
34
35
36
37
38
39
40
41
42
43
44
45
46
47
48
49
50
51
52
53
54
55
56
57
58
59
60
61
62
63
64
65

112 soil is different than that of a saturated soil, and that it will gradually converge with the virgin
113 compression line of saturated soil at high stresses with an intersection point dependent on the initial
114 degree of saturation. Nonetheless, similar to Uchaipichat and Khalili (2009), Mun and McCartney
115 (2016) found that the virgin compression lines for specimens with different initial degrees of
116 saturation in effective stress space were relatively parallel for mean effective stresses less than 3
117 MPa, which is in the stress range relevant to most geotechnical applications. Instead of changing
118 the slope of the virgin compression lines for unsaturated soils, Khalili et al. (2004) found that the
119 collapse phenomenon may be captured by considering the relative changes in preconsolidation
120 stress and effective stress with changes in degree of saturation or suction. This may imply that a
121 linkage between the LC curve and the compression curve may not be necessary in all effective
122 stress-based elasto-plastic frameworks.

123 A remaining issue in the definition of the LC curve is confirmation of the role of hydraulic
124 hysteresis on the yield stress evolution during wetting and drying, and understanding the situations
125 in which it needs to be considered. In field applications such as slopes and pavements, for example,
126 wetting and drying may lead to hysteretic changes in stiffness that may lead to temporal variations
127 in deformations. Romero and Jommi (2008) noted that irreversible strains could be observed
128 following a wetting-drying path using a suction-controlled oedometer under isotropic conditions
129 and Khosravi and McCartney (2012) showed that hysteretic changes in the small strain shear
130 modulus during drying and wetting may be linked to hysteretic changes in the preconsolidation
131 stress. Further, hydraulic hysteresis may be encountered when loading soil under undrained
132 drainage conditions, where a change in degree of saturation and suction are expected during
133 compression, as will be discussed later in this paper. Although there have been several hydro-
134 mechanical frameworks proposed to account for changes in the yield stress during wetting or

1
2
3
4 135 drying (Wheeler et al. 2003; Tamagnini 2004; Sun et al. 2008, Sheng et al. 2004), they have not
5
6
7 136 been used to evaluate the impact of hydraulic hysteresis for soils compressed under different
8
9 137 drainage conditions. Accordingly, the objective of this paper is to provide a simple approach to
10
11
12 138 investigate the evolution of the mean effective preconsolidation stress with degree of saturation
13
14 139 using a linkage to the shape of the SWRC.

16 140 **CALIBRATION OF THE PRECONSOLIDATION STRESS RELATIONSHIP**

19 141 The hysteretic preconsolidation stress relationship proposed in this study couples the LC curve
20
21 142 relationship of Salager et al. (2008) with the van Genuchten (1980) SWRC relationship to predict
22
23
24 143 a non-linear relationship between the preconsolidation stress and the matric suction normalized by
25
26 144 the air entry suction. The SWRC during hydraulic hysteresis is typically defined using a primary
27
28
29 145 drying path that governs the drainage process from a water-saturated soil, a primary wetting curve
30
31 146 that governs the wetting process from an air-dry soil, and scanning curves that transition between
32
33
34 147 the primary wetting and drying curves depending on the initial state of an unsaturated soil
35
36 148 undergoing a wetting or drying process. The van Genuchten (1980) SWRC model for the primary
37
38 149 drying path is given as follows:

$$S_r = S_{res} + (1 - S_{res}) \left[\frac{1}{1 + (\alpha_{vG} \cdot \psi)^{n_{vG}}} \right]^{\frac{1}{1-n_{vG}}} \quad (1)$$

46 150 where S_{res} is the residual degree of saturation and α_{vG} and n_{vG} are fitting parameters. The approach
47
48
49 151 used to simulate hydraulic hysteresis in this study was to fit a modified version of the van
50
51 152 Genuchten (1980) SWRC to the wetting path data from the experimental studies, which includes
52
53
54 153 a scanning curve and a portion of the primary wetting path. The equation used in this case is:

$$S_r = (S_{\max} - S_{\min}) \cdot \left[\frac{1}{1 + (\alpha_{vG} \cdot \psi)^{n_{vG}}} \right]^{\frac{1}{1-n_{vG}}} \quad (2)$$

154 where S_{\max} is the maximum degree of saturation on the primary wetting curve and S_{\min} is the degree
 155 of saturation on the drying curve at the point of wetting. This approach provides a good fit to
 156 measured wetting path data but does not provide a generalized model for predicting any hysteretic
 157 path. Alternative approaches to capture the hysteretic SWRC are to assume a piece-wise log-linear
 158 SWRC (Wheeler et al. 2003), linear scanning curve connecting the primary drying and wetting
 159 paths (Tamagnini 2004), or modification of the parameters from the primary drying path to predict
 160 the wetting path (Kool and Parker 1987). Nonetheless, the approach using Equation (2) permits a
 161 simple evaluation of linkages between the SWRC and the preconsolidation stress that is the focus
 162 of this study.

163 It should be noted that hydraulic hysteresis can be influenced by the initial conditions. For
 164 example, Della Vecchia et al. (2013) reported a different primary wetting path for different void
 165 ratios. Although differences may exist between the SWRC (and the air entry suction) at different
 166 stresses during compression or for soils with different initial densities, the effect of these factors
 167 are neglected in this study for simplicity. As compression of soils will change the pore structure
 168 and thus the SWRC, the stress-dependent SWRC model of Zhou and Ng (2014) can be
 169 incorporated into a relationship for the preconsolidation stress. However, there is insufficient data
 170 to apply the relationship from this Zhou and Ng (2014) at the current time.

171 When interpreting the preconsolidation stress, the mean effective stress was evaluated using
 172 the definition of generalized effective stress proposed by Bishop and Blight (1963), as follows:

$$p' = p_{net} + \chi \psi \quad (3)$$

1
2
3
4 173 where p_{net} is mean net stress, ψ is the matric suction equal to the difference between the pore
5
6
7 174 air pressure u_a and the pore water pressure u_w , and χ is the effective stress parameter assumed to
8
9
10 175 be equal to the degree of saturation S_r for simplicity. Many other choices are available for the
11
12 176 definition of the value of χ , including the effective saturation (Bolzon and Schrefler 1995; Lu et
13
14 177 al. 2010), a function of the air entry suction (Khalili and Khabbaz 1998), and experimental shear
15
16
17 178 strength data (Lu and Likos 2006; Khalili and Zargarbashi 2010).

18
19 179 Salager et al. (2008) proposed a semi-logarithmic relationship to capture the association
20
21
22 180 between p'_c and ψ as follows:

$$\frac{p'_c(\psi)}{p'_c(\psi=0)} = \begin{cases} 1 & \text{if } \psi \leq \psi_{ae} \\ 1 + \gamma_\psi \log \frac{\psi_0}{\psi_{ae}} & \text{if } \psi > \psi_{ae} \end{cases} \quad (4)$$

23
24
25
26
27
28
29
30 181 where $p'_c(\psi)$ and $p'_c(\psi=0)$ are the values of mean effective preconsolidation stress at matric
31
32 182 suctions of ψ and zero, respectively, ψ_{ae} is the air entry suction, and γ_ψ is a material parameter that
33
34
35 183 defines the impact of matric suction on p'_c . The relationship assumes a piecewise log-linear
36
37 184 relationship for the SWRC where no change in degree of saturation occurs until the applied matric
38
39
40 185 suction has surpassed the air entry suction. Therefore, no changes in p'_c will occur until $\psi > \psi_{ae}$.
41
42 186 The relationship of Salager et al. (2008) has been adopted by several constitutive frameworks to
43
44
45 187 define the LC curve in the $p' - \psi$ space (François and Laloui 2008; Bellia et al. 2015).

46
47 188 A potential drawback of the relationship of Salager et al. (2008) involves the “if” statement
48
49
50 189 required to maintain a constant value for p'_c while $\psi \leq \psi_{ae}$, and the fact that there is not data
51
52 190 showing the evolution in p'_c for suctions less than the ψ_{ae} . In order to predict the trends in
53
54
55 191 preconsolidation stress and degree of saturation, the model of Salager et al. (2008) was modified
56
57 192 to relate p'_c and S_r as follows:

$$\frac{p'_c(S_r)}{p'_c(S_r=1)} = \begin{cases} 1 & \text{if } \psi \leq \psi_{ae} \\ 1 + \gamma_\psi \log \left[\left(\frac{1}{\alpha_{vG}} \left\{ \frac{1}{(S_e)^{1-n_{vG}}} - 1 \right\}^{\frac{1}{n_{vG}}} \right) \times \frac{1}{\psi_{ae}} \right] & \text{if } \psi > \psi_{ae} \end{cases} \quad (5)$$

where γ_ψ is the same soil parameter from the relationship between suction and p'_c , and S_e is the effective degree of saturation defined as $(S_r - S_{res}) / (1 - S_{res})$.

Data sets available in the literature that involve information on the role of suction and degree of saturation on the hardening response of unsaturated soils were selected to calibrate the hysteretic preconsolidation stress relationships in Equations (4) and (5). The calibration was restricted to studies that involved the drained, isotropic compression of soils that had experienced different hydraulic testing paths before loading. Uchaipichat and Khalili (2009) performed suction controlled isotropic loading tests on a compacted silt for different values of matric suction (0, 100, and 300 kPa) while Uchaipichat (2010) investigated the influence of hydraulic hysteresis on the compression curve and preconsolidation stress for different values of matric suction. Coccia (2016) investigated the impact of degree of saturation on the mean effective preconsolidation stress of compacted silt using a high pressure thermal isotropic cell. Khosravi et al. (2016) performed a series of isotropic compression tests to represent the impact of suction-induced hardening on the dynamic shear modulus of unsaturated soils. The data of Salager et al. (2008) was not included in this evaluation because of the large variability observed in the reported preconsolidation stress trends with suction. Other studies such as Mun and McCartney (2015, 2016) present drained compression curves for specimens with different initial suction values, but the specimens were prepared using different compaction efforts and may have different soil structures that may influence the preconsolidation stress.

1
2
3
4 212 The first step in evaluating the hysteretic preconsolidation stress model was to determine the
5
6
7 213 parameters α_{vG} and n_{vG} for different soils from the literature using least squares minimization.
8
9 214 Drying-path SWRCs collected from the literature are shown in Figure 2(a). Using the method of
10
11
12 215 least squares, the preconsolidation stresses from Equation (5) calculated from the value of degree
13
14 216 of saturation at the point of yielding are compared with the measured values of p'_c for each test in
15
16
17 217 Figure 2(b). A good match between the experimental preconsolidation stress values and the results
18
19 218 from Equation (5) is obtained in this figure. The evolution of p'_c as a function of the initial suction
20
21
22 219 (ψ_0) and normalized initial suction (ψ_0/ψ_{ae}) for these soils calculated using Equation (4) are shown
23
24 220 in Figures 2(c) and 2(d), respectively. The relationship also provides a reasonable match to the
25
26
27 221 preconsolidation stress in terms of suction for the four soils.

28
29 222 The preconsolidation stress values for compacted Kaolinite specimens that had experienced a
30
31
32 223 wetting and drying path before undergoing isotropic, drained compression reported by Uchaipichat
33
34 224 (2010) are investigated in Figure 3. To identify the effect of S_r on p'_c by incorporating the hysteretic
35
36 225 SWRC, the van Genuchten (1980) SWRC model parameters were determined for the primary
37
38
39 226 drying and wetting paths shown in Figure 3(a). The changes in p'_c with S_r obtained from Equation
40
41
42 227 (5) are shown in Figure 3(b), and changes in p'_c with ψ_0 and ψ_0/ψ_{ae} obtained from Equation (4) are
43
44 228 shown in Figures 3(c) and 3(d), respectively. The values of p'_c were not observed to exhibit any
45
46
47 229 significant change with matric suction during hydraulic hysteresis in Figures 3(c) and 3(d), while
48
49 230 a clear hysteretic trend between p'_c and S_r was observed in Figure 3(b) for specimens that had
50
51 231 previously experienced drying or wetting paths. Although the comparison in Figure 3 indicates
52
53
54 232 that it may be simpler to use the relationship between the preconsolidation stress and suction (Fig.
55
56 233 3(c)) in hydro-mechanical frameworks due to the lack of hysteresis in this relationship, there are
57
58
59 234 hydro-mechanical paths where the suction and degree of saturation may both change, such as

1
2
3
4
5
6
7
8
9
10
11
12
13
14
15
16
17
18
19
20
21
22
23
24
25
26
27
28
29
30
31
32
33
34
35
36
37
38
39
40
41
42
43
44
45
46
47
48
49
50
51
52
53
54
55
56
57
58
59
60
61
62
63
64
65

235 undrained compression (i.e., compression under constant water content conditions). In this case, it
236 may be easier to track or estimate changes in the degree of saturation, and use the hysteretic
237 relationship in Equation (5) to predict the preconsolidation stress. In this case, the relationship in
238 terms of degree of saturation in Figure 3(b) may be more useful. Although not shown here,
239 Khosravi et al. (2016) also presented a single preconsolidation stress value for a specimen that had
240 been wetted following a drying path, and similar observations to those in Figure 3 were drawn.

241 There are several other studies that have evaluated the compression of unsaturated soils under
242 undrained (or constant water content) conditions (e.g., Jotisankasa et al. 2007; Sun et al. 2008;
243 Della Vecchia et al. 2013). In these cases, the suction and degree of saturation need to be monitored
244 or inferred during compression in order to perform an effective stress analysis, as both variables
245 can change during undrained compression. Of the studies provided above, Jotisankasa (2005) and
246 Jotisankasa et al. (2007) provided sufficient information to perform this analysis and evaluate the
247 hysteretic preconsolidation stress relationship. The measured drying and wetting path SWRCs
248 from Jotisankasa (2005) and Jotisankasa et al. (2007) along with van Genuchten (1980) SWRC
249 fitting parameters are shown in Figure 4(a), while a comparison between the preconsolidation
250 stress data from their undrained compression tests and the fitted relationship from Equation (5) is
251 shown in Figure 4(b). A value of γ_ψ of 19.0 was identified for the compacted silty clay using least
252 squares minimization, which was greater than that observed in the other studies presented in Table
253 1 and likely reflects soil- and test-specific conditions. Nonetheless, a good fit is observed between
254 the experimental data and the model. The trends in preconsolidation stress with ψ and ψ/ψ_{ac} from
255 Equation (4) are shown in Figure 4(c) and 4(d), and a good match is also observed with the model.

1
2
3
4 256 **APPLICATION OF THE PRECONSOLIDATION STRESS MODEL IN PREDICTING**
5
6
7 257 **COMPRESSION RESPONSE UNDER DIFFERENT DRAINAGE CONDITIONS**
8

9 258 The compression of soils under either undrained or drained conditions can be considered to
10
11 259 elucidate how the hysteretic preconsolidation stress model may be used in different situations.
12
13
14 260 During drained compression, the suction will remain constant while the degree of saturation will
15
16 261 increase as the voids are compressed. The only way for the suction to remain constant but for the
17
18
19 262 degree of saturation to increase would be for the shape of the SWRC to change, as shown in
20
21 263 Figure 5(a) for a hypothetical soil. In this case, it may be simplest to estimate the preconsolidation
22
23
24 264 stress in terms of suction using Equation (4), as shown in Figure 5(b). During undrained
25
26 265 compression, it is expected that the degree of saturation will increase and the suction will decrease
27
28
29 266 during undrained compression, as shown in Figure 5(c) for a hypothetical soil. The degree of
30
31 267 saturation is likely proportional to the change in volume of the soil and may be easy to estimate
32
33
34 268 using a model such as that of Zhou et al. (2012b). However, the change in suction may not be
35
36 269 simple to estimate as the shape of the SWRC is likely changing. In addition to this, the model in
37
38 270 Equation (4) does not capture the preconsolidation stress variation during the increase in degree of
39
40
41 271 saturation during compression, so Equation (4) may not be suitable to predict the evolution in
42
43 272 preconsolidation stress during undrained compression. In this case, it may be best to estimate the
44
45
46 273 preconsolidation stress defined in Equation (5) using estimates of the degree of saturation during
47
48 274 compression, as shown in Figure 5(d). It is acknowledged that the magnitude of changes in degree
49
50
51 275 of saturation and suction are not as significant before the applied mean stress reaches the
52
53 276 preconsolidation stress as they may be for higher stresses (Wheeler et al. 2003). Nonetheless, the
54
55 277 nonlinear trends between preconsolidation stress and degree of saturation from the proposed
56
57
58 278 relationship indicate that this still may be important to consider.
59
60
61
62
63
64
65

1
2
3
4 279 To evaluate the situations described in the previous paragraph quantitatively, the proposed
5
6 280 preconsolidation stress models in Equations (4) and (5) can be utilized alongside a simple elasto-
7
8
9 281 plastic model to predict the compression curves of soils during drained compression using the
10
11 282 relationship between preconsolidation stress and suction, and to predict the compression curves of
12
13
14 283 soils during undrained (constant water content) compression using the wetting-path relationship
15
16 284 between preconsolidation stress and the degree of saturation. The compression curves from the
17
18
19 285 experiments indicate that the unsaturated soils exhibit elastic behavior until reaching a mean
20
21 286 effective preconsolidation stress p'_c . In the elastic region, changes in void ratio (e) up p'_c can be
22
23
24 287 expressed as follows:

$$\Delta e = \kappa \cdot \ln \frac{p'_f}{p'_0} \quad p'_f < p'_c \quad (6)$$

25
26
27
28
29
30 288 where p'_0 and p'_f are the initial and final mean effective stresses, and p'_c is the mean effective
31
32
33 289 preconsolidation stress, which can be predicted by using either Equations (4) or (5). The value of
34
35 290 κ is assumed to be constant regardless of the initial suction or initial degree of saturation.
36
37

38 291 After reaching the mean apparent preconsolidation stress, the unsaturated specimens are
39
40 292 assumed to decrease in volume irrespective of suction magnitudes or degree of saturation. The
41
42
43 293 compression response of unsaturated soils for stresses greater than p'_c can be calculated as follows:
44
45

$$\Delta e = \lambda \cdot \ln \frac{p'_f}{p'_0} \quad p'_c < p'_0 < p'_f \quad (7)$$

46
47
48
49
50 294 where λ is the slope of the VCL for unsaturated soil and is assumed to be constant for unsaturated
51
52
53 295 soils over the stress range of interest to geotechnical problems following the observations of
54
55 296 Uchaipichat and Khalili (2009) and Mun and McCartney (2015). Although the slope λ for
56
57
58 297 unsaturated soils is assumed to be the same regardless of the suction, it is assumed to be greater
59
60
61
62
63
64
65

1
2
3
4
5
6
7
8
9
10
11
12
13
14
15
16
17
18
19
20
21
22
23
24
25
26
27
28
29
30
31
32
33
34
35
36
37
38
39
40
41
42
43
44
45
46
47
48
49
50
51
52
53
54
55
56
57
58
59
60
61
62
63
64
65

298 than or equal than the slope λ_0 for saturated soil in the mean effective stress range relevant to
299 geotechnical engineering problems. This follows the observations of several experimental studies
300 (i.e., Sivakumar 1993; Uchaipichat and Khalili 2009; Mun and McCartney 2015).

301 Zhou et al. (2012a) introduced an expression to predict the change in the effective saturation
302 caused by suction and stress changes by using a hydro-mechanical interaction function (D_e).
303 However, the model of Zhou et al. (2012a) has a limitation in the evaluation of compression
304 behavior with the change of suction or degree of saturation because of the complexity in
305 calculation methods. Sun et al. (2008) also suggested an analytical expression to predict the change
306 of degree of saturation and suction through inclusion of hydraulic hysteresis during undrained
307 compression. This study employed a simplified approach to predict the change of degree of
308 saturation during undrained compression based on the assumption that the variation in the degree
309 of saturation of unsaturated soil is directly related to the changes in void ratio, an approach used
310 by Jotisankasa (2005) and Jotisankasa et al. (2007). Changes in degree of saturation during initial
311 compression in the elastic region can be calculated as follows:

$$\Delta S_r = \kappa \cdot \ln \frac{p'_f}{p'_0} \quad p'_f < p'_c \quad (8)$$

312 The changes in degree of saturation can be used in an incremental form to calculate changes in the
313 mean effective preconsolidation stress using Equation (5). Although not as critical to this study
314 but still relevant for calculation of the mean effective stress using Equation (3), the degree of
315 saturation for stresses greater than p'_c can be calculated as follows:

$$\Delta S_r = \lambda \cdot \ln \frac{p'_f}{p'_c} \quad p'_c < p'_0 < p'_f \quad (9)$$

1
2
3
4 316 **VALIDATION OF THE PRECONSOLIDATION STRESS MODEL IN PREDICTING**
5
6
7 317 **COMPRESSION CURVES**
8

9 318 In order to verify the simple elasto-plastic framework together with the hysteretic
10
11 319 preconsolidation stress model, comparisons between the simulated and measured compression
12
13
14 320 curves for drained compression tests presented by Uchaipichat (2010) and undrained compression
15
16 321 tests presented by Jotisankasa et al. (2007) are shown in Figures 6(a) and 6(b), respectively. In
17
18
19 322 addition to the values of γ_v defined in Figures 3 and 4 for each of the two studies respectively, the
20
21 323 parameters of the framework were calibrated to predict the compression curves of the two
22
23
24 324 unsaturated soils under different initial conditions, and are summarized in Table 2. Further, the
25
26 325 actual initial conditions (e.g., $S_{r,0}$, e_0 , p') from the experiments shown in Table 2 were used as
27
28
29 326 inputs. The simulated compression curves appear to match well with the experimental compression
30
31 327 behavior in Figures 6(a) and 6(b), and capture the different suction hardening effects for the
32
33
34 328 specimens tested in both drained and undrained conditions.

35
36 329 The approach described in Figures 5(a) and 5(b) was used to simulate the drained compression
37
38 330 data of Uchaipichat (2010) while the approach described in Figures 5(c) and 5(d) was used to
39
40
41 331 simulate the undrained compression data of Jotisankasa et al. (2007). Uchaipichat (2010) did not
42
43 332 report the change of degree of saturation during drained compression, which required an estimated
44
45
46 333 trend in S_r to calculate the mean effective stress. Although Equations (8) and (9) are meant for use
47
48 334 in estimating changes in degree of saturation in undrained compression tests, they were used to
49
50
51 335 predict the change of degree of saturation during compression under constant suction conditions,
52
53 336 as shown in Figure 6(c). On the other hand, Jotisankasa et al. (2007) reported changes in degree
54
55
56 337 of saturation and suction during undrained compression, and the data in Figure 6(d) indicates that
57
58 338 the degree of saturation calculated using Equations (8) and (9) matches the data well. Although
59
60
61
62
63
64
65

1
2
3
4
5
6
7
8
9
10
11
12
13
14
15
16
17
18
19
20
21
22
23
24
25
26
27
28
29
30
31
32
33
34
35
36
37
38
39
40
41
42
43
44
45
46
47
48
49
50
51
52
53
54
55
56
57
58
59
60
61
62
63
64
65

339 the degree of saturation only increases by about 2% during the elastic loading for the different
340 specimens, this small change still causes a relevant decrease in preconsolidation stress of about 6
341 to 10% due to the steep shape of the wetting path curve in Figure 4(b). The suction values used in
342 the simulation of the data of Uchaipichat are shown in Figure 6(e), and are constant as the test is
343 drained. The suction values used in the simulation of the data from Jotisankasa et al. (2007) were
344 estimated from the calculated values of S_r using the SWRC for simplicity, and the comparison in
345 Figure 6(f) indicates a good fit with most of the measured suction values in the tests.

346 The values of preconsolidation stress for the drained tests of Uchaipichat (2010) obtained from
347 the suction values in Figure 6(e) using Equation (4) lead to a good fit to the experimental
348 preconsolidation stress values as shown in Figure 6(g). As expected, the preconsolidation stress is
349 constant during drained compression. In Figure 6(g), the point of yielding is reflected by the
350 intersection between the preconsolidation stress line and the 1:1 line. The trends in
351 preconsolidation stress for the undrained tests of Jotisankasa et al. (2007) obtained from the degree
352 of saturation trends in Figure 6(d) using Equation (5) are shown in Figure 6(h). A decreasing trend
353 in preconsolidation stress during compression is observed due to the reduction in S_r . The slope of
354 the trend in preconsolidation stress increases with increasing suction due to the nonlinearity in the
355 hysteretic preconsolidation stress relationship.

356 The comparison in Figure 6 shows conceptually how the hysteretic preconsolidation stress
357 relationship described by Equations (4) and (5) can be applied for different hydro-mechanical
358 paths. Although the changes in degree of saturation in the elastic zone are expected to be the same
359 due to the use of the same value of κ in Equation (8), the shape of the SWRC may lead to different
360 impacts of this change in degree of saturation on the predicted preconsolidation stress
361 relationships. This also indicates that the shape of the SWRC for a given soil may have an impact

1
2
3
4
5
6
7
8
9
10
11
12
13
14
15
16
17
18
19
20
21
22
23
24
25
26
27
28
29
30
31
32
33
34
35
36
37
38
39
40
41
42
43
44
45
46
47
48
49
50
51
52
53
54
55
56
57
58
59
60
61
62
63
64
65

362 on how important hydraulic hysteresis may be in predicting the compression curve in undrained
363 conditions.

364 **CONCLUSIONS**

365 This paper proposes a mean effective preconsolidation stress relationship that describes
366 evolution in this variable with the suction and degree of saturation during hydraulic hysteresis,
367 which was validated based on available data sets in the literature. The relationship was then used
368 in a simple, effective stress-based elasto-plastic framework to predict the compression curves of
369 soils during drained compression (constant suction) using the relationship between
370 preconsolidation stress and suction, and to predict the compression curves of soils during
371 undrained (constant water content) compression using the wetting-path relationship between
372 preconsolidation stress and the degree of saturation. The proposed relationship was found to
373 satisfactorily capture the relative changes in preconsolidation stress with suction and degree of
374 saturation, and was shown to be useful to simulate the compression curves of unsaturated soils
375 under different drainage conditions and corresponding hydro-mechanical paths.

376 **ACKNOWLEDGEMENTS**

377 The authors appreciate the support from National Science Foundation grant CMMI-1054190.
378 The views in this paper are those of the authors alone.

379 **REFERENCES**

380 Alonso, E.E., Gens, A., and Josa, A. (1990). "A constitutive model for partially saturated soils."
381 Géotechnique. 40(3), 405-430.
382 Alsherif, N.A., and McCartney, J.S. (2016). "Yielding of silt at high temperature and suction
383 magnitudes." Geotechnical and Geological Engineering. 34, 501-514.

1
2
3
4
5
6
7
8
9
10
11
12
13
14
15
16
17
18
19
20
21
22
23
24
25
26
27
28
29
30
31
32
33
34
35
36
37
38
39
40
41
42
43
44
45
46
47
48
49
50
51
52
53
54
55
56
57
58
59
60
61
62
63
64
65

384 Bellia, Z., Ghembaza, M.S., and Belal, T. (2015). “A thermo-hydro-mechanical model of
385 unsaturated soils based on bounding surface plasticity.” *Computers and Geotechnics*. 69, 58-
386 69.

387 Bishop, A.W., and Blight, G.E. (1963). “Some aspects of effective stress in saturated and
388 unsaturated soils.” *Géotechnique*. 13(3), 177–197.

389 Bolzon, G., and Schrefler, B.A. (1995). “State surfaces of partially saturated soils: an effective
390 pressure approach.” *Applied Mechanics Reviews*. 48(10), 643-649.

391 Coccia, C.J.R. (2016). *Mechanisms of Thermal Volume Change in Unsaturated Silt*. Ph.D. Thesis.
392 University of Colorado, Boulder.

393 Cui, Y.J., Delage, P., and Sultan, N. (1995). “An elastoplastic model for compacted soils.”
394 *Proceedings of 1st International Conference on Unsaturated Soils, Paris, France*, Alonzo, E.
395 E., and Delage, P., eds., Balkema, Rotterdam, The Netherlands, 2, 703-709.

396 Della Vecchia, G., Jommi, C., and Romero, E. (2013). “A fully coupled elastic-plastic hydro-
397 mechanical model for compacted soils accounting for clay activity.” *International Journal for*
398 *Numerical and Analytical Methods in Geomechanics*. 37(5), 503-535.

399 François, B., and Laloui, L. (2008). “ACMEG-TS: A constitutive model for unsaturated soils under
400 non-isothermal conditions.” *International Journal for Numerical and Analytical Methods in*
401 *Geomechanics*. 32(16), 1955-1988.

402 Gallipoli, D., Wheeler, S.J., and Karstunen, M. (2003). “Modelling the variation of degree of
403 saturation in a deformable unsaturated soil.” *Géotechnique*. 53(1), 105-112.

404 Geiser, F., Laloui, L., and Vulliet L. (2006). “Elasto-plasticity of unsaturated soils: laboratory test
405 results on a remoulded silt.” *Soils and Foundations*. 46(5), 545-556.

1
2
3
4
5
6
7
8
9
10
11
12
13
14
15
16
17
18
19
20
21
22
23
24
25
26
27
28
29
30
31
32
33
34
35
36
37
38
39
40
41
42
43
44
45
46
47
48
49
50
51
52
53
54
55
56
57
58
59
60
61
62
63
64
65

406 Jotisankasa, A., Ridley, A., and Coop, A. (2007). "Collapse behavior of a compacted silty clay in
407 the suction-monitored oedometer apparatus." *Journal of Geotechnical and Geoenvironmental*
408 *Engineering*, 133(7), 867-877

409 Khalili, N. and Khabbaz, M.H. (1998). "A unique relationship for χ for the determination of shear
410 strength of unsaturated soils." *Géotechnique*. 48(5), 681–688,

411 Khalili, N., Geiser, F., and Blight, G.E. (2004). "Effective stress in unsaturated soils, a review with
412 new evidence." *International Journal of Geomechanics*. 4(2), 115-126.

413 Khalili, N., Habte, M.A., and Zargarbashi, S. (2008). "A fully coupled flow deformation model
414 for cyclic analysis of unsaturated soils including hydraulic and mechanical hysteresis."
415 *Computers and Geotechnics* 35, 872–889.

416 Khalili, N. and Zargarbashi, S. (2010). "Influence of hydraulic hysteresis on effective stress in
417 unsaturated soils." *Géotechnique*. 60(9), 729-734.

418 Khosravi, A. and McCartney, J.S. (2012). "Impact of hydraulic hysteresis on the small-strain shear
419 modulus of unsaturated soils." *Journal of Geotechnical and Geoenvironmental Engineering*.
420 138(11), 1326–1333.

421 Khosravi, A., Sajjad, S., Dadashi, A., and McCartney, J.S. (2016). "Evaluation of the impact of
422 drainage-induced hardening on the small strain shear modulus of unsaturated soils."
423 *International Journal of Geomechanics*. 1-10. 10.1061/(ASCE)GM.1943-5622.0000614.

424 Kool, J.B. and Parker, J.C. (1987). "Development and evaluation of closed-form expressions for
425 hysteretic soil hydraulic properties." *Water Resource Research*. 23(1), 105-114.

426 Lloret, A., Villar, M.V., Sanchez, M., Gens, A., Pintado, X., and Alonso, E.E. (2003). "Mechanical
427 behaviour of heavily compacted bentonite under high suction changes," *Géotechnique*. 53(1),
428 27-40.

1
2
3
4
5
6
7
8
9
10
11
12
13
14
15
16
17
18
19
20
21
22
23
24
25
26
27
28
29
30
31
32
33
34
35
36
37
38
39
40
41
42
43
44
45
46
47
48
49
50
51
52
53
54
55
56
57
58
59
60
61
62
63
64
65

429 Loret, B. and Khalili, N. (2002). “An effective stress elastic-plastic model for unsaturated porous
media.” *Mechanics of Materials*. 34(2), 97-116.

431 Lu, N. and Likos, W.J. (2006), Suction stress characteristic curve for unsaturated soil, *J. Geotech.
Geoenviron. Eng.*, 132(2), 131-142.

433 Lu, N., Godt, J., and Wu, D. (2010). “A closed-form equation for effective stress in unsaturated
soil.” *Water Res. Res.*, 46, 1–14.

435 Mun, W., and McCartney, J.S. (2015). “Compression mechanisms of unsaturated clay under high
stress levels.” *Canadian Geotechnical Journal*. 52(12), 2099-2112.

437 Mun, W. and McCartney, J.S. (2016). “Constitutive model for the drained compression of
unsaturated clay to high stresses.” *ASCE Journal of Geotechnical and Geoenvironmental
Engineering*. 04017014-11-11. 10.1061/(ASCE)GT.1943-5606.0001662.

440 Romero, E., and Jommi, C. (2008). “An insight into the role of hydraulic history on the volume
changes of anisotropic clayey soils.” *Water Resources Research*, 44, W12412:1-W12412:16

442 Salager, S., François, B., El Youssoufi, M.S., Laloui, L. and Saix, C. (2008). “Experimental
investigations of temperature and suction effects on compressibility and pre-consolidation
pressure of a sandy silt.” *Soils and Foundations*. 48(4): 453-466.

445 Sheng, D., Sloan, S., Gens, A. (2004). “A constitutive model for unsaturated soils:
thermomechanical and computational aspects.” *Computational Mechanics*, 33, 453-465.

447 Sun, D.A., Sheng, D., Xiang L., Sloan S.W. (2008). “Elastoplastic prediction of hydro-mechanical
behaviour of unsaturated soils under undrained conditions.” *Computers and Geotechnics*. 35,
845-852.

450 Tamagnini R. (2004). “An extended Cam-clay model for unsaturated soils with hydraulic
hysteresis.” *Géotechnique*. 54(3), 223-228.

1
2
3
4
5
6
7
8
9
10
11
12
13
14
15
16
17
18
19
20
21
22
23
24
25
26
27
28
29
30
31
32
33
34
35
36
37
38
39
40
41
42
43
44
45
46
47
48
49
50
51
52
53
54
55
56
57
58
59
60
61
62
63
64
65

452 Tourchi, S., and Hamidi, A. (2015). "Thermo-mechanical constitutive modeling of unsaturated
453 clays based on the critical state concepts." *Journal of Rock Mechanics and Geotechnical*
454 *Engineering*. 7(2), 193-198.

455 Uchaipichat, A. and Khalili, N. (2009). "Experimental investigation of thermo-hydro-mechanical
456 behaviour of an unsaturated silt." *Géotechnique*. 59(4), 339-353.

457 Sivakumar, V. (1993). *A Critical State Framework for Unsaturated Soils*. Ph.D. Thesis. University
458 of Sheffield.

459 Uchaipichat, A. (2010). "Hydraulic hysteresis effect on compressibility of unsaturated soils."
460 *ARNP Journal of Engineering and Applied Science*. 5(10), 92-97.

461 van Genuchten, M.T. (1980). "A closed form equation for predicting the hydraulic conductivity of
462 unsaturated soils." *Soil Science Society of America Journal*. 44(5), 892-898.

463 Wheeler, S.J. and Sivakumar, V. (1995). "An elasto-plastic critical state framework for unsaturated
464 soils." *Géotechnique*. 45(1), 35-53.

465 Wheeler, S.J., Gallipoli, D., and Karstunen, M. (2002). "Comments on the use of Barcelona Basic
466 Model for unsaturated soils." *International Journal for Numerical and Analytical Methods in*
467 *Geomechanics*. 26, 1561-1571

468 Wheeler, S.J., Sharma, R.J. and Buisson, M.S.R. (2003). "Coupling of hydraulic hysteresis and
469 stress-strain behaviour in unsaturated soils." *Géotechnique*. 53(1), 41-54.

470 Wood, D.M. (1990). *Soil Behaviour and Critical State Soil Mechanics*. Cambridge University
471 Press. New York, United States.

472 Zhou, A.-N., Sheng, D., Sloan, S.W., and Gens, A. (2012a). "Interpretation of unsaturated soil
473 behaviour in the stress – saturation space, I: Volume change and water retention behavior."
474 *Computers and Geotechnics*. 43: 178-187.

1
2
3
4
5
6
7
8
9
10
11
12
13
14
15
16
17
18
19
20
21
22
23
24
25
26
27
28
29
30
31
32
33
34
35
36
37
38
39
40
41
42
43
44
45
46
47
48
49
50
51
52
53
54
55
56
57
58
59
60
61
62
63
64
65

475 Zhou, A-N., Sheng, D., Sloan, S.W., and Gens, A. (2012b). “Interpretation of unsaturated soil
476 behaviour in the stress – saturation space, II: Constitutive relationships and validations.”
477 Computers and Geotechnics. 43, 111-123.

478 Zhou, C., and Ng, C.W.W. (2014). “A new and simple stress-dependent water retention model for
479 unsaturated soil.” Computers and Geotechnics. 62, 216-222.

480

1
2
3
4 481 **LIST OF TABLE AND FIGURE CAPTIONS**

5
6 482 **TABLE 1.** Parameters of the preconsolidation stress model for different soils

7
8
9 483 **TABLE 2.** Calibrated parameters for the simulated compression curves of soils loaded in drained
10
11 and undrained conditions
12 484

13
14 485 **FIG. 1:** Various LC curves as defined by: (a) Alonso et al. (1990); (b) Salager et al. (2008);
15
16 486 (c) Turchi and Hamidi (2015); (d) Wheeler et al. (2003); (e) Zhou et al. (2012a)

17
18
19 487 **FIG. 2:** Normalized mean effective preconsolidation stress for specimens loaded in drained
20
21 488 compression after following a drying path for different soils from the literature: (a) SWRCs;
22
23 489 (b) Variation with initial degree of saturation; (c) Variation with initial matric suction;
24
25 490 (d) Variation with normalized initial matric suction

26
27
28
29 491 **FIG. 3:** Normalized mean effective preconsolidation stress for specimens loaded in drained
30
31 492 compression after following drying-wetting paths (data from Uchaipichat 2010): (a) SWRCs;
32
33 493 (b) Variation with initial degree of saturation; (c) Variation with initial matric suction;
34
35 494 (d) Variation with normalized initial matric suction

36
37
38 495 **FIG. 4:** Normalized mean effective preconsolidation stress for specimens loaded in undrained
39
40 496 compression after following compaction-wetting paths (data from Jotisankasa 2005 and
41
42 Jotisankasa et al. 2007): (a) SWRCs; (b) Variation with initial degree of saturation; (c)
43 497 Variation with initial matric suction; (d) Variation with normalized initial matric suction

44
45 498
46
47
48 499 **FIG. 5:** Role of drainage conditions during compression: (a) SWRC wetting paths during drained
49
50 500 compression; (b) Preconsolidation stress prediction during drained compression; (c) SWRC
51
52 wetting paths during undrained compression; (d) Preconsolidation stress prediction during
53 501 undrained compression
54
55 502

1
2
3
4
5
6
7
8
9
10
11
12
13
14
15
16
17
18
19
20
21
22
23
24
25
26
27
28
29
30
31
32
33
34
35
36
37
38
39
40
41
42
43
44
45
46
47
48
49
50
51
52
53
54
55
56
57
58
59
60
61
62
63
64
65

FIG. 6: Comparison of the model calibration (dashed lines) with the experimental data for drained [Uchaipichat 2010] and undrained [Jotisankasa 2005; Jotisankasa et al. 2007] compression: (a) $e\text{-log}p'$ (drained); (b) $e\text{-log}p'$ (undrained); (c) Degree of saturation values predicted (drained); (d) Degree of saturation values predicted (undrained); (e) Suction change during compression (drained); (f) Suction change during compression (undrained); (g) Preconsolidation stress evolution during compression (drained); (h) Preconsolidation stress evolution during compression (undrained)

1
2
3
4
5
6
7
8
9
10
11
12
13
14
15
16
17
18
19
20
21
22
23
24
25
26
27
28
29
30
31
32
33
34
35
36
37
38
39
40
41
42
43
44
45
46
47
48
49
50
51
52
53
54
55
56
57
58
59
60
61
62
63
64
65

511 **TABLE 1:** Parameters of the preconsolidation stress relationship for different soils

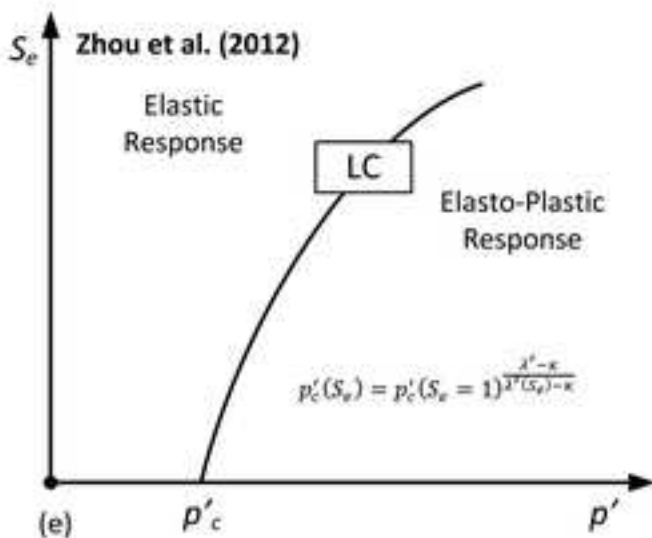
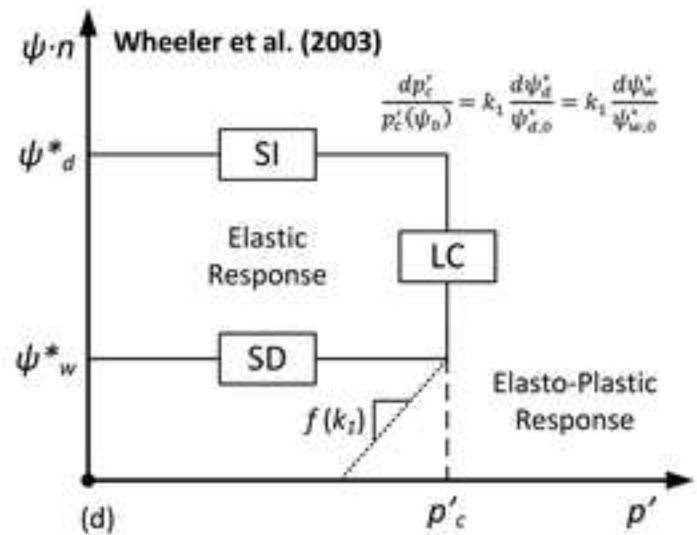
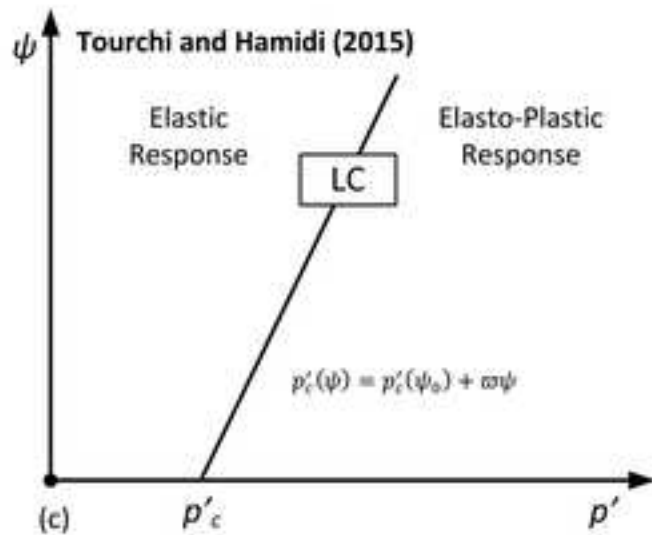
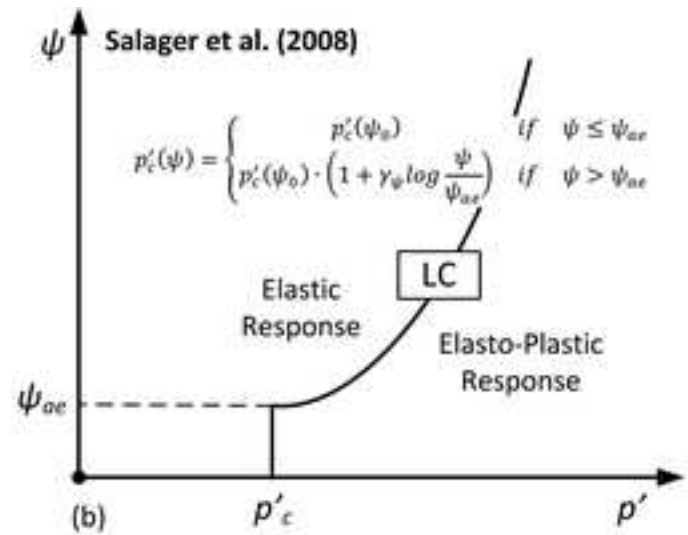
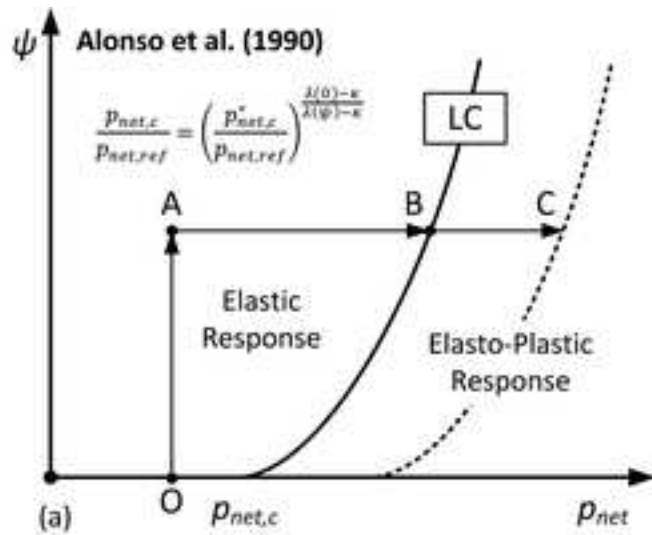
Study	Soils investigated	Drying-path SWRC model parameters (van Genuchten 1980)				p' _c relationship parameter
		α_{vg} (kPa ⁻¹)	n_{vg}	$S_{r,min}$	Ψ_{ae} (kPa)	γ_{ψ}
Coccia (2016)	Compacted Bonny silt	0.16	1.38	0.03	2	0.765
Khosravi et al. (2016)	Compacted Bonny silt	0.02	2.60	0.06	10	0.700
Uchaipichat (2010)	Compacted Kaolinite	0.002	1.49	0.00	25	0.700
Uchaipichat & Khalili (2010)	Compacted Bourke silt	0.03	3.15	0.03	18	0.197

512
513 **TABLE 2:** Calibrated parameters for the simulated compression curves of soils loaded in drained
514 and undrained conditions

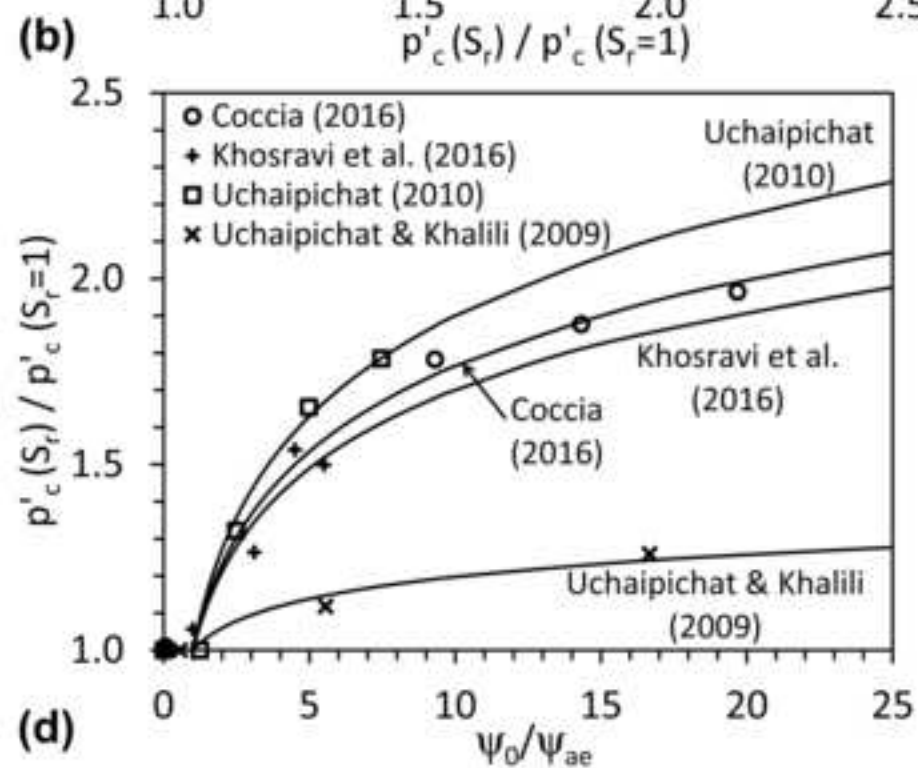
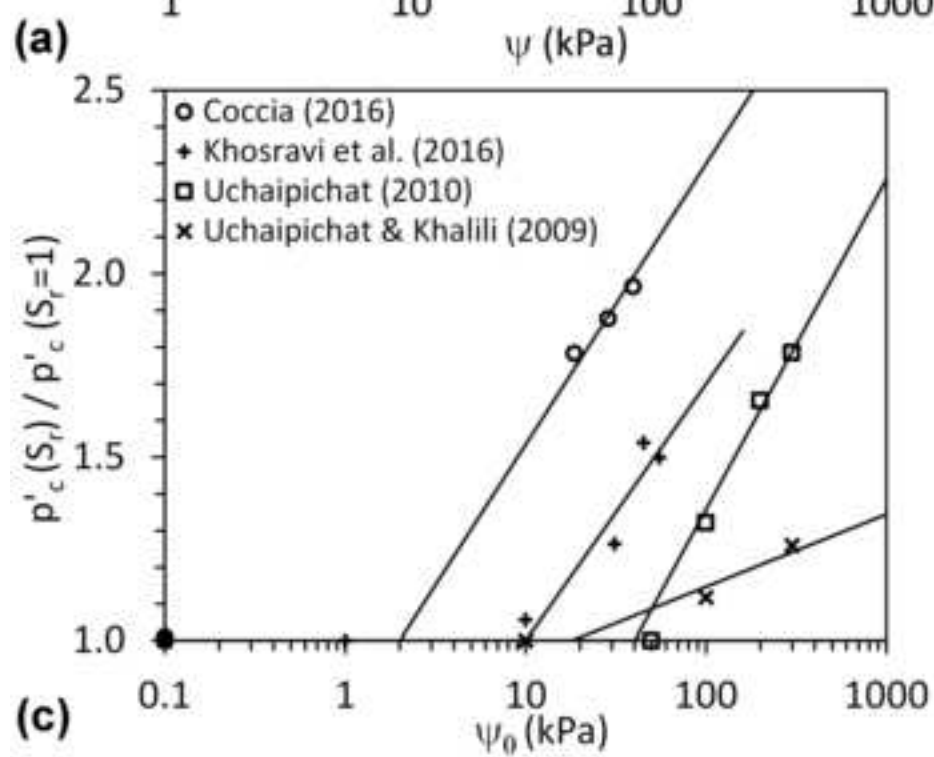
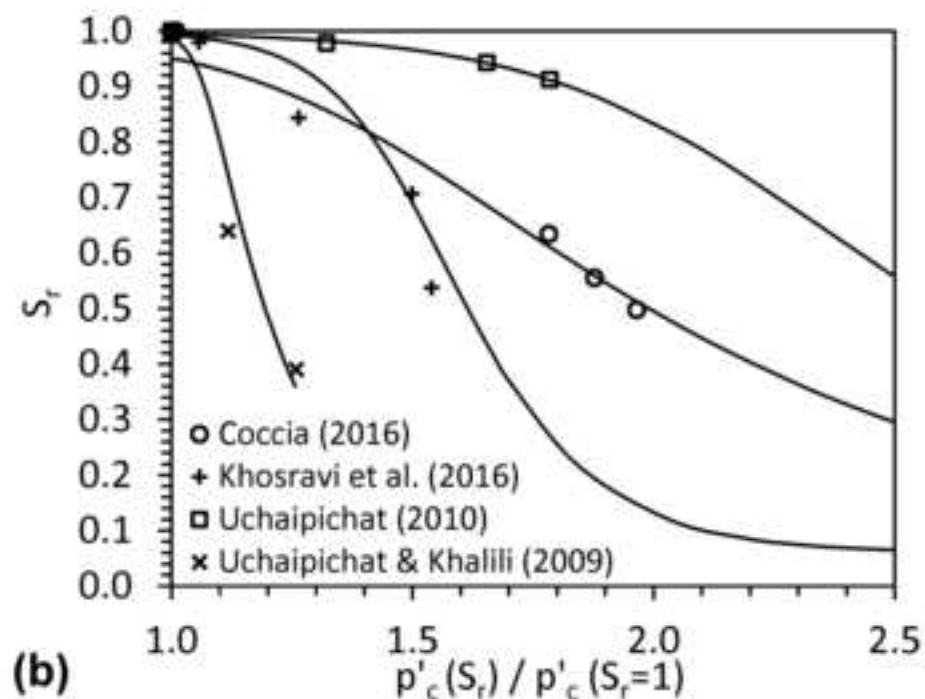
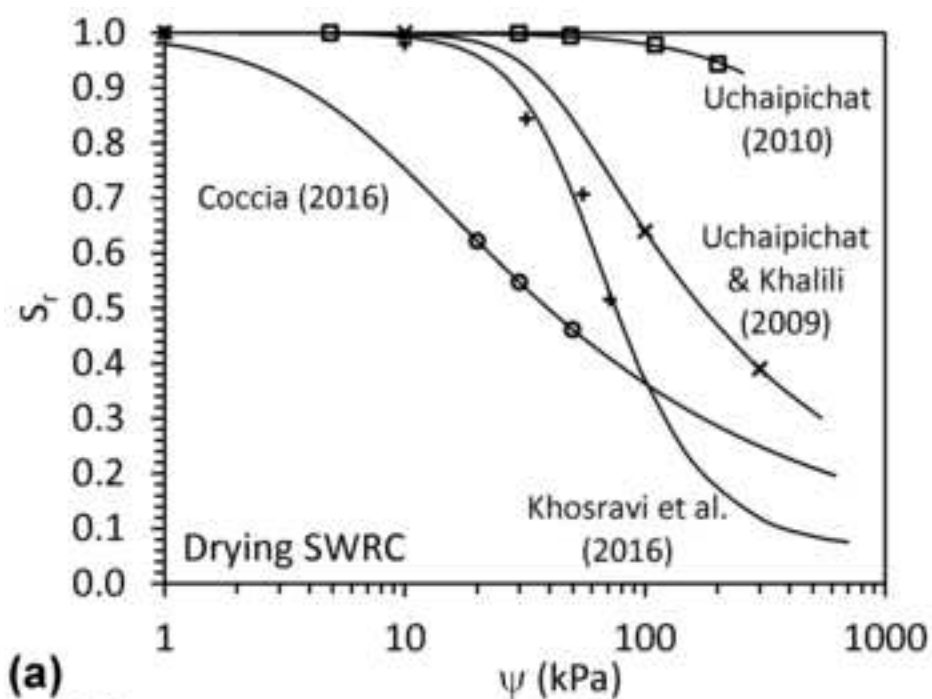
Variable	Drained condition (Uchaipichat 2010)	Undrained condition (Jotisankasa 2005; Jotisankasa et al. 2007)
Initial suctions evaluated, ψ_0 (kPa)	0 / 50 / 100 / 200 / 300	0 / 75 / 134 / 525 / 936
Initial degrees of saturation evaluated, $S_{r,0}$	1.00 / 0.97 / 0.96 / 0.95 / 0.91	1.00 / 0.54 / 0.49 / 0.40 / 0.36
Initial void ratios evaluated, e_0	1.05 / 1.04 / 1.04 / 1.03 / 1.03	0.71 / 0.71 / 0.71 / 0.70 / 0.69
λ_0 (Saturated)	0.065	0.086
λ (Unsaturated)	0.070	0.178
κ	0.005	0.007
Ψ_{ae} (kPa)	25.0	45.0
α_{vg} (kPa ⁻¹)	0.019	0.095
n_{vg}	3.60	1.65
$S_{r,max}$	0.994	0.982
$S_{r,min}$ (the same for all tests)	0.912	0.365
p' _c relationship parameter, γ_{ψ}	0.7	19.0

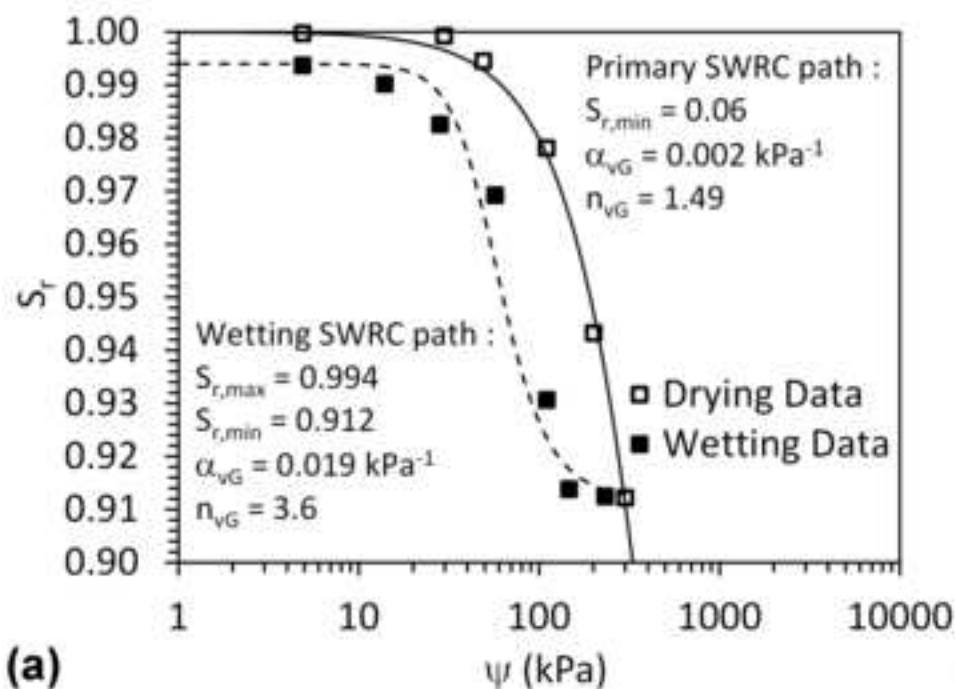
515

516

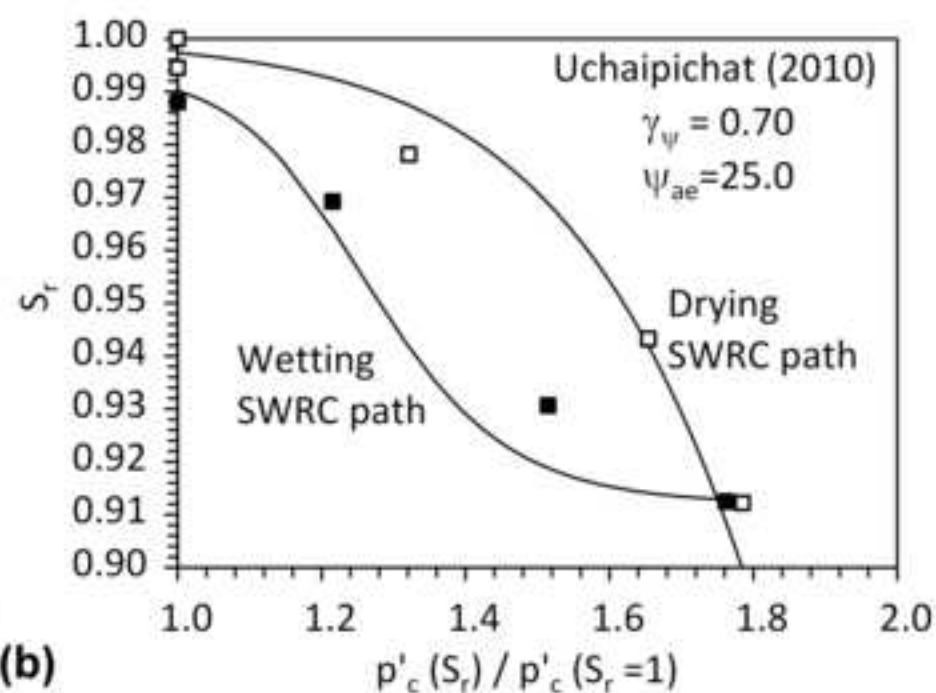


$p_{net,ref}$ - reference stress state; $p_{net,c}$ - preconsolidation stress; ψ - matric suction; $p'_{net,c}$ - preconsolidation stress at saturation soil conditions; $\lambda(\psi)$ - slope of the isotropic virgin compression line in the mean net stress space; $\lambda(\psi)$ - slope of the isotropic virgin compression line for saturated soil; κ - slope of the recompression line; $p'_c(\psi)$ - mean effective preconsolidation stress at ψ ; $p'_c(\psi_0)$ - mean effective preconsolidation stress at matric suction, ψ_0 (typically 0); ψ_{oe} - air entry value of matric suction; γ_w - material parameter that defines the relative impact of matric suction on p'_c ; ω - dimensionless parameter which defines the linear variation of p'_c with ψ ; $\psi_{d,0}^*$ - modified suction limits of the suction increase (SI) curve; $\psi_{w,0}^*$ - modified suction limits of the suction decrease (SD) curve; k_1 - defines the relative path traced by the corners of the LC and SI/SD curves during yielding; S_e - effective degree of saturation; $p'_c(S_e)$ - apparent mean effective preconsolidation stress at S_e ; $\lambda'(S_e)$ - slope of the isotropic effective virgin compression line at S_e .

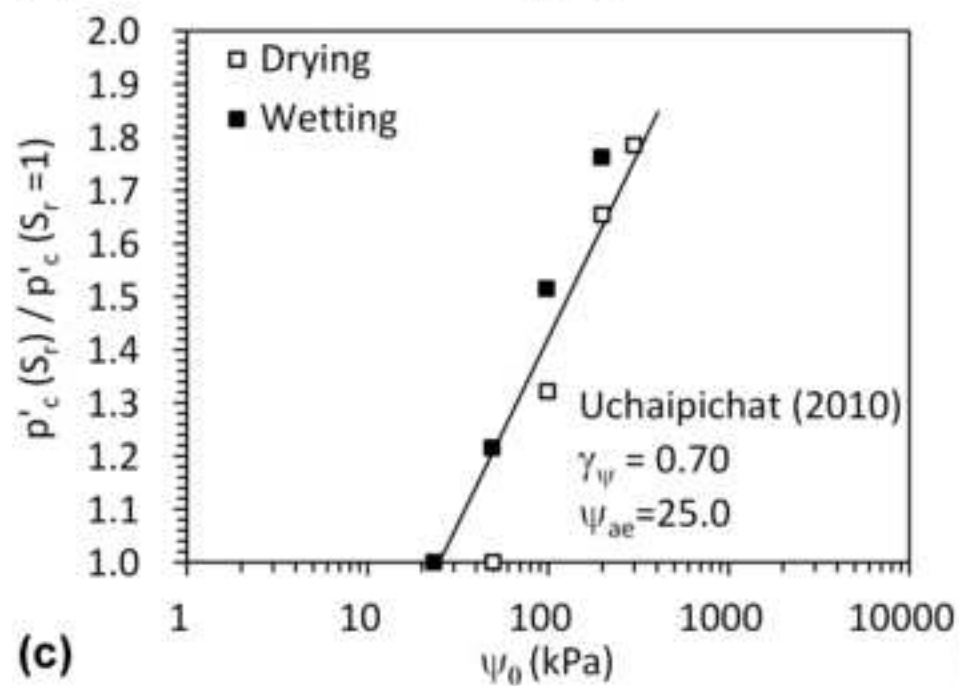




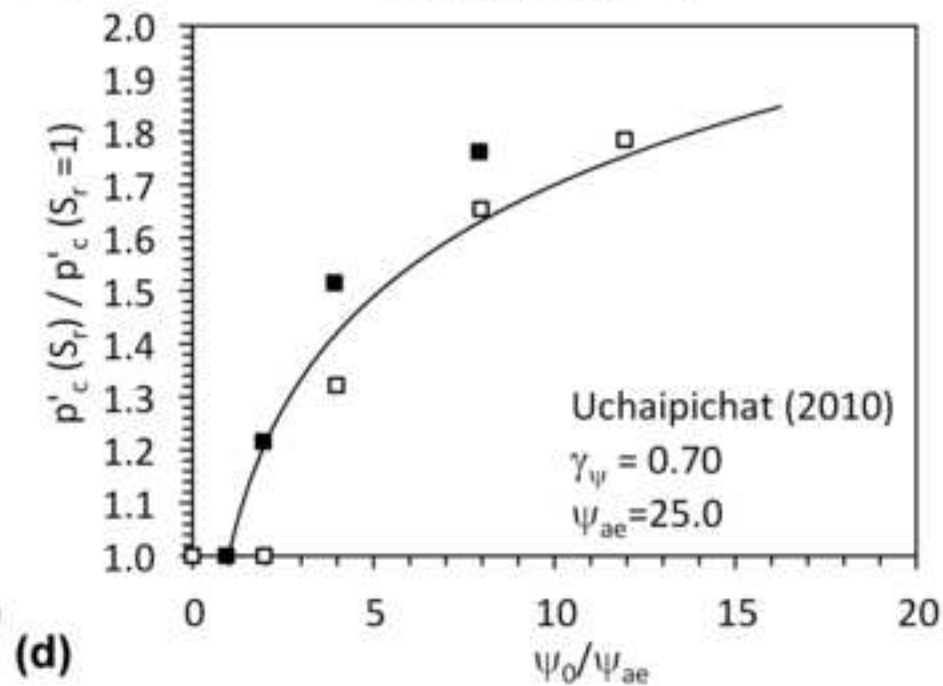
(a)



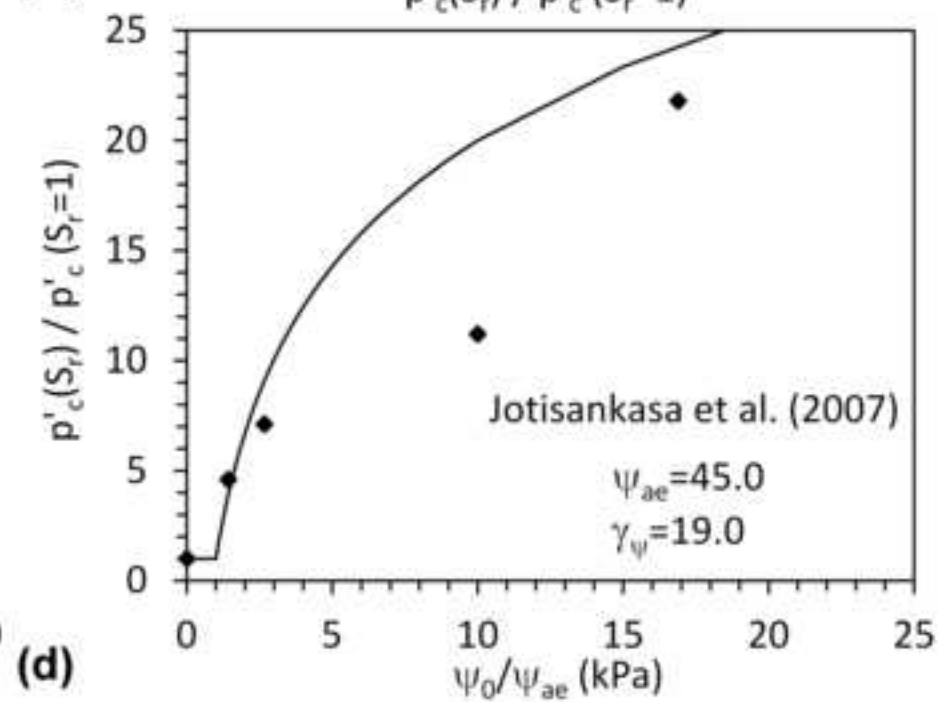
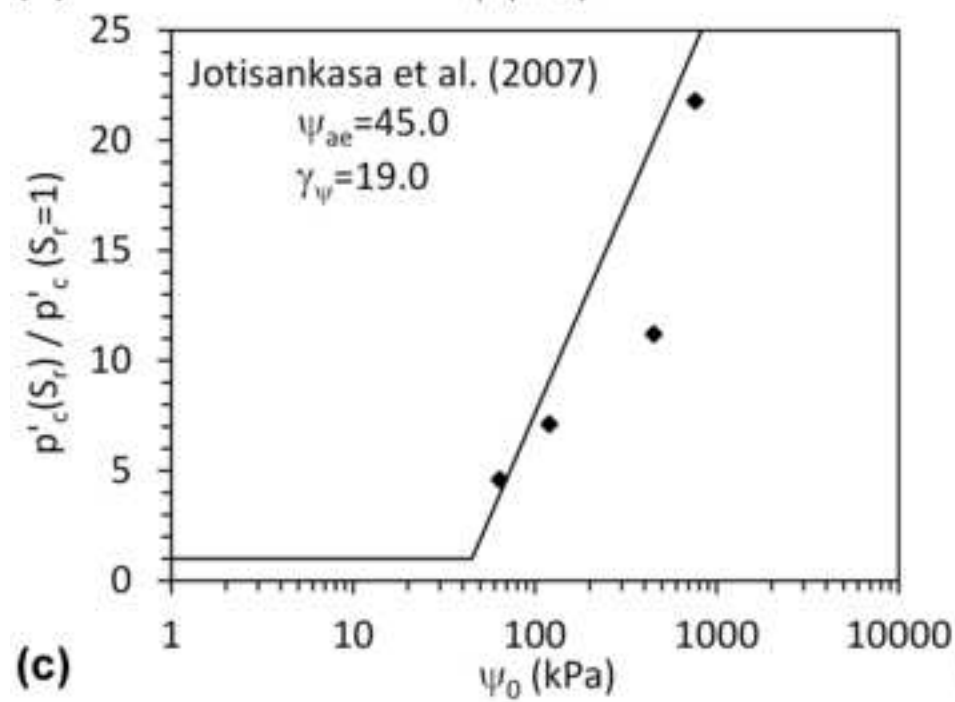
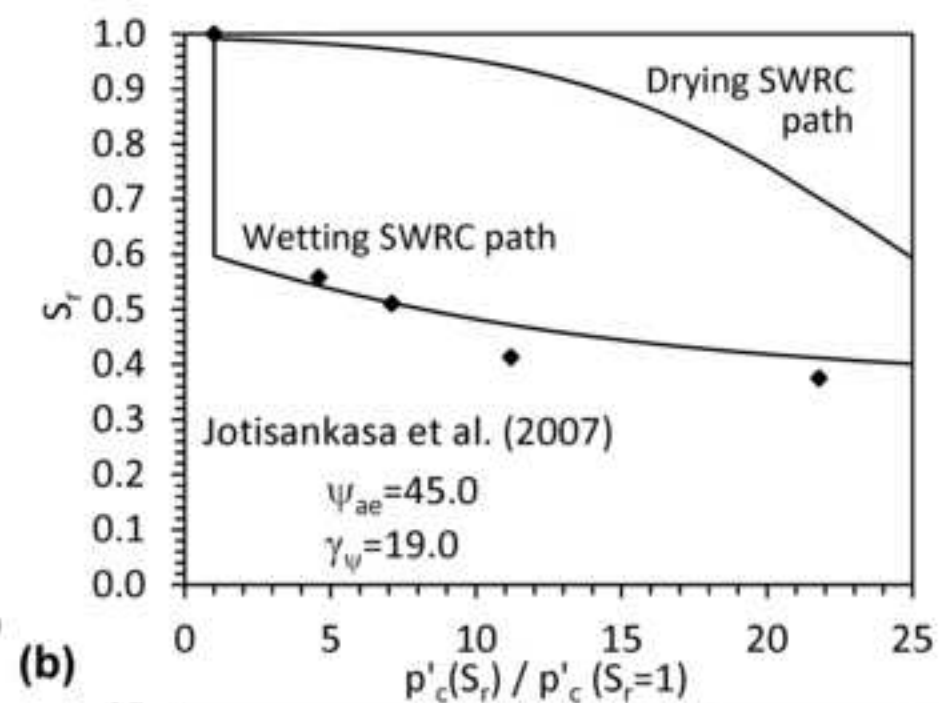
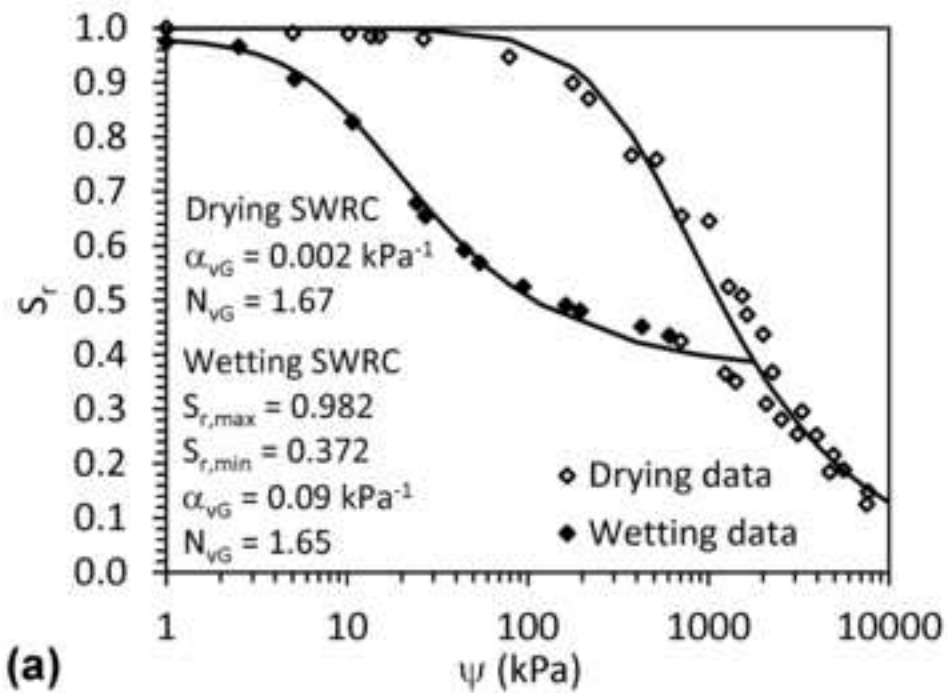
(b)

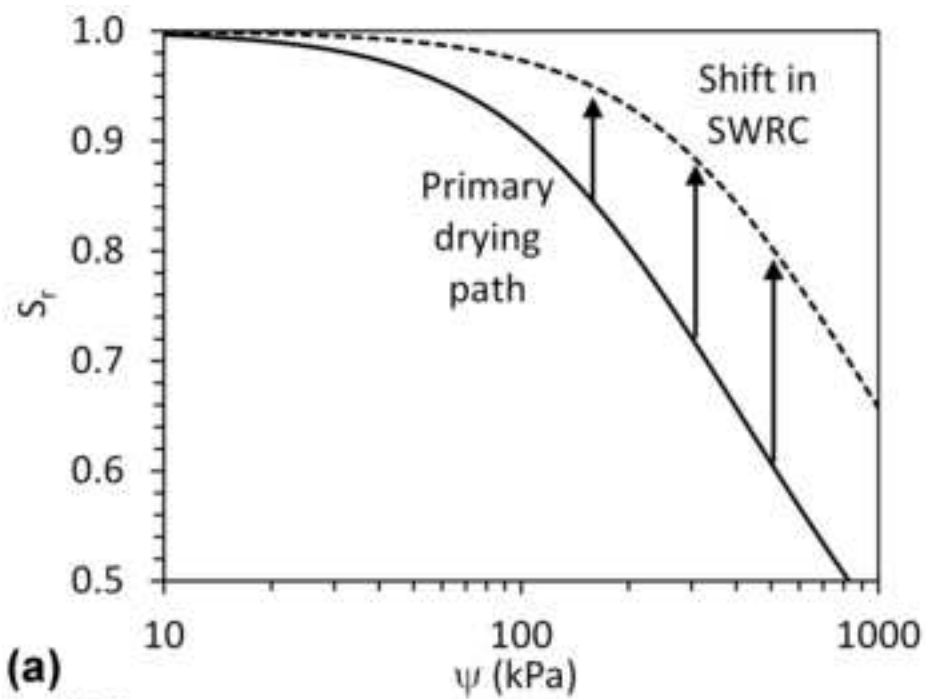


(c)

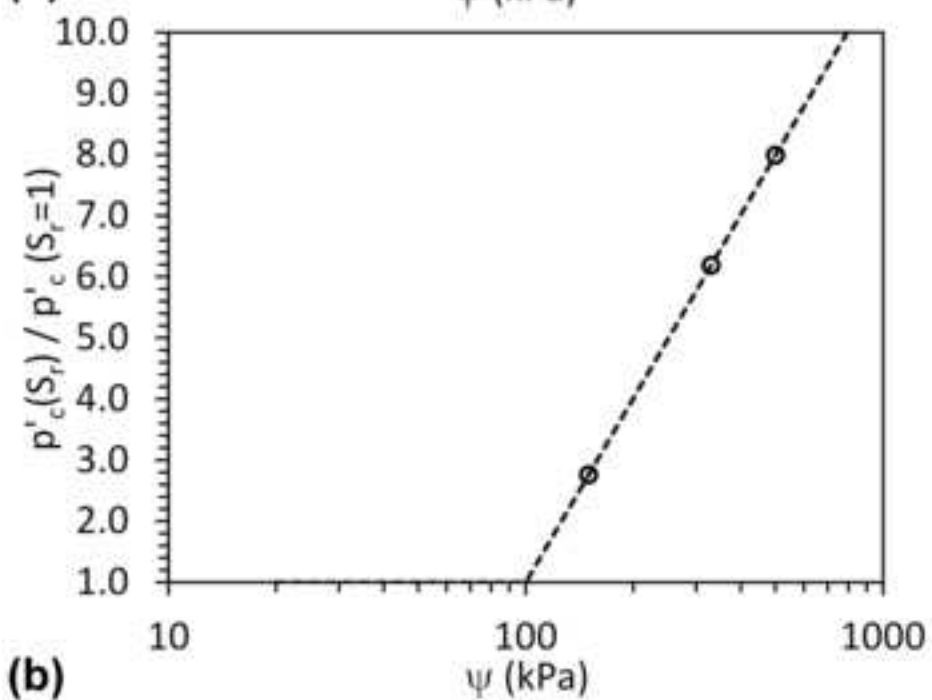


(d)

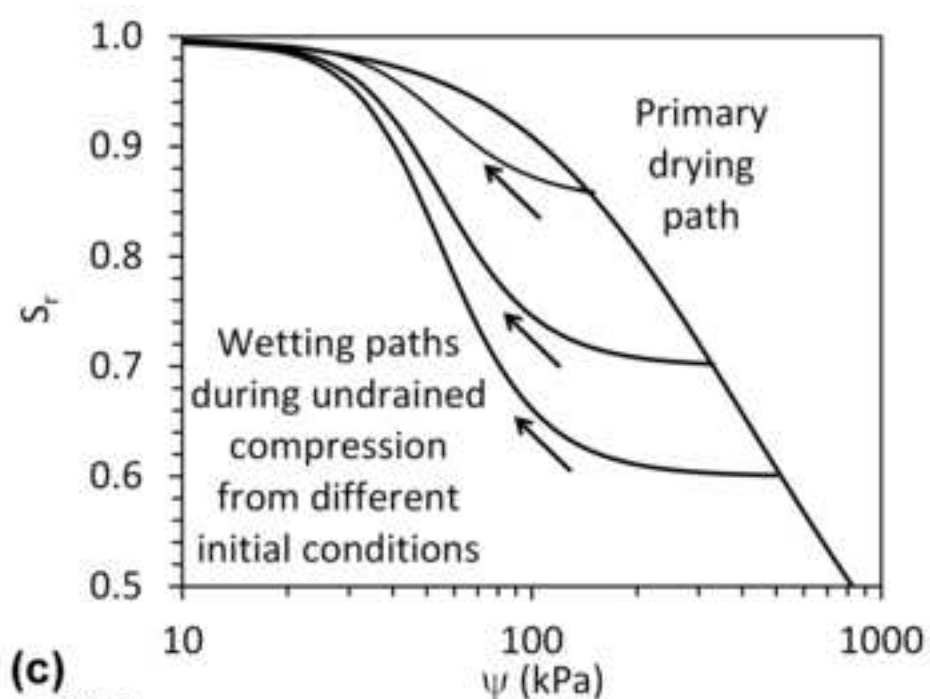




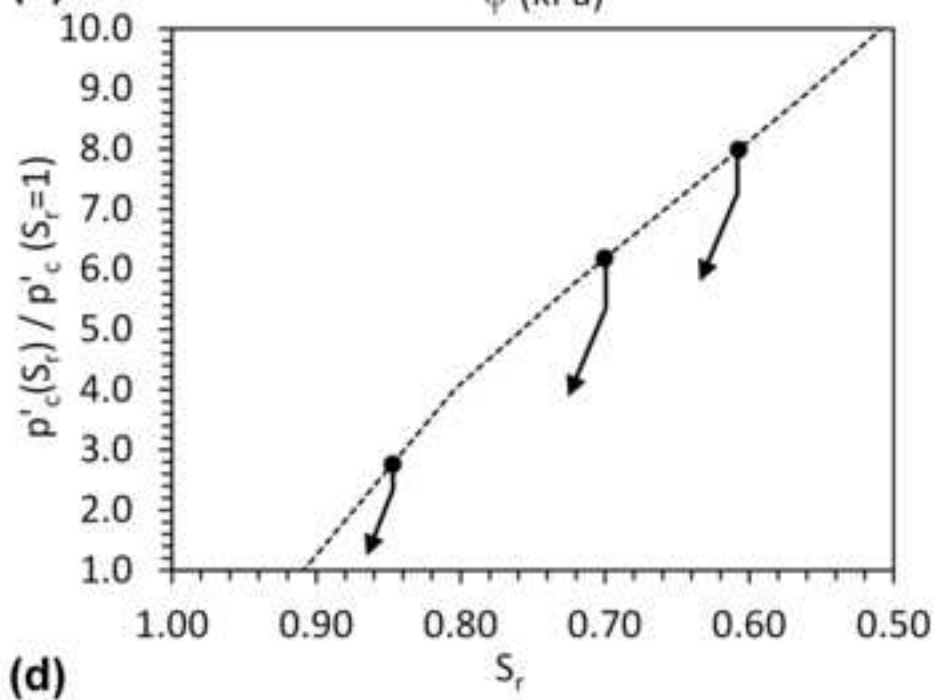
(a)



(b)



(c)



(d)

